

Pentapertetrahedral Clusters as Building Blocks for a Three-Dimensional Sulfide Superlattice**

Nanfeng Zheng, Xianhui Bu, and Pingyun Feng*

Chalcogenides are becoming increasingly important in the development of new solid-state materials for technological applications. Chalcogenide clusters with well-defined size and composition represent the lower limit of semiconducting nanoparticles and serve to span the size gap between quantum dot structures and molecular species in solution.^[1] Moreover, these large clusters can be used as building blocks to construct supramolecular assemblies with unique properties. Among chalcogenide clusters with various geometrical features,^[2–4] tetrahedral clusters are of particular significance because they can act as pseudotetrahedral building blocks for the construction of zeolite-like open architectures.^[5–9] Unfortunately, even though a number of superlattices built from super-tetrahedral clusters have been reported,^[10–13] relatively little progress has been made with other types of tetrahedral clusters.

Here we report a three-dimensional open-framework material (denoted ICF-26) built from an unusual tetrahedral cluster. ICF-26 was prepared from the Ca–Li–In–S quaternary system in a procedure mimicking the preparation of natural zeolites by using alkali and alkaline earth metal cations as structure-directing agents.^[14] Organic species are not needed as either surface-stabilizing ligands or extraframework structure-directing agents, in contrast to other recent work that relies heavily on the use of organic compounds.^[15–21] The highly mobile extraframework cations results in the ionic conductivity of ICF-26 being higher than that of any previously known crystalline lithium compound at room temperature.^[22,23]

ICF-26 is built from a tetrahedral cluster denoted P2 (Figure 1). The P2 cluster (that is, $\text{Li}_4\text{In}_{22}\text{S}_{44}^{18-}$) is the second member of a mathematical series of pentapertetrahedral clusters P_n , thus termed because they can be conceptually constructed by coupling four supertetrahedral clusters onto the faces of an antipertetrahedral cluster of the same order (Figure 1). Supertetrahedral clusters are regular tetrahedron-

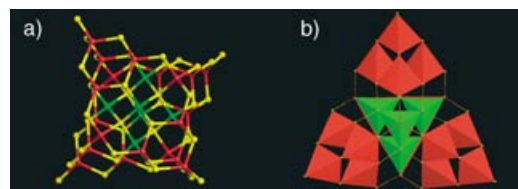


Figure 1. a) Ball-and-stick view of the P2 cluster $\text{Li}_4\text{In}_{22}\text{S}_{44}^{18-}$. Red: In^{3+} , green: mixed $\text{In}^{3+}/\text{Li}^+$ sites, yellow: S^{2-} . b) Four supertetrahedral T2 clusters (red) are covalently bonded to one antipertetrahedral T2 cluster (green) to form a pentapertetrahedral P2 cluster in ICF-26.

shaped fragments of the cubic ZnS type lattice and are denoted as T_n , where n is the number of metal layers.^[10] An antipertetrahedral cluster is defined here as having the same geometrical features as a supertetrahedral cluster with the positions of cations and anions being exchanged.

Thus, the P1 cluster consists of four T1 clusters (MX_4) at the corners and one anti-T1 cluster (XM_4) at the core, resulting in the composition $(\text{MX}_4)_4(\text{XM}_4)$ (namely, M_8X_{17}). Examples of P1 clusters include $[\text{SCd}_8(\text{SBu})_{12}](\text{CN})_{4/2}$, $\text{K}_{10}\text{M}_4\text{Sn}_4\text{S}_{17}$ ($\text{M} = \text{Mn, Fe, Co, Zn}$), and $[\text{M}_4(\text{Se})(\text{SnSe}_4)_4]^{10-}$ ($\text{M} = \text{Zn, Mn}$).^[24–26] The P2 cluster contains four T2 clusters (M_4X_{10}) and one anti-T2 cluster (X_4M_{10}), thus giving the composition $(\text{M}_4\text{X}_{10})_4(\text{X}_4\text{M}_{10})$ (namely, $\text{M}_{26}\text{X}_{44}$; Figure 1). The P3 cluster (not yet synthesized) consists of four T3 clusters ($\text{M}_{10}\text{X}_{20}$) and one anti-T3 cluster ($\text{X}_{10}\text{M}_{20}$) with the composition $(\text{M}_{10}\text{X}_{20})_4(\text{X}_{10}\text{M}_{20})$ (namely, $\text{M}_{60}\text{X}_{90}$). The same procedure can be used to derive the composition of other P_n clusters.

A pentapertetrahedral cluster is considerably larger than a supertetrahedral cluster of the same order, and hence it is difficult to prepare open-framework materials with pentapertetrahedral clusters larger than P1. Even though supertetrahedral clusters as large as T5 are known,^[12] the P2 cluster reported herein represents the largest known cluster of the P_n series.

While all metal cations of each P2 cluster adopt tetrahedral coordination, sulfur atoms can be two-, three-, or four-coordinate. There are a total of four tetrahedrally coordinated sulfur atoms. They are tetrahedrally distributed around the geometrical center of the P2 cluster and are in fact the anionic core of the anti-T2 cluster. To satisfy Pauling's electrostatic valence rule,^[12,27] each tetrahedral S^{2-} site is surrounded by two Li^+ and two In^{3+} sites to give a bond valence sum of +2, which is consistent with the valence of S^{2-} . There are three statistically equivalent ways to achieve this when two In^{3+} and four Li^+ cations are placed at six core cationic sites. As a result, all six metal sites of the anti-T2 clusters are disordered with each site occupied by 2/3 Li^+ cations and 1/3 In^{3+} cations (Figure 1). This leads to an overall cluster formula of $\text{Li}_4\text{In}_{22}\text{S}_{44}^{18-}$. The corner sharing of S sites results in the overall framework composition being $\text{Li}_4\text{In}_{22}\text{S}_{42}^{14-}$, which is consistent with both the elemental analysis and the crystallographic occupancy refinement.^[14] The crystallographically determined formula is $\text{Li}_{4.13}\text{In}_{21.9}\text{S}_{42}$. Similar tetrahedral coordination of Li to S is known in a number of other sulfides such as Li_2S (2.47 Å), KLiMnS_2 (2.44 Å), and LiGaS_2 (2.29–2.59 Å).^[28–30] The Li–S bond length in the tetrahedral

[*] N. Zheng, Prof. P. Feng
Department of Chemistry
University of California
Riverside, California 92521 (USA)
Fax: (+1) 909-787-4713
E-mail: pingyun.feng@ucr.edu

Prof. X. Bu
Department of Chemistry and Biochemistry
California State University
1250 Bellflower Blvd.
Long Beach, CA 90840 (USA)

[**] We are grateful for the support of CSULB (X.B.), the National Science Foundation (DMR-0349326, P.F.), Beckman Foundation (P.F.), and the donors of the Petroleum Research Fund (administered by the ACS, P.F.). P.F. is an Alfred P. Sloan research fellow.

environment matches well with the In–S distance in these clusters (about 2.4 Å).

The topological type of ICF-26 resembles that of the cubic ZnS lattice (Figure 2). Even with the formation of two interpenetrating lattices, the framework of ICF-26 is still highly open. More than half of the crystal volume (58.8%) is occupied by extraframework species in ICF-26, as calculated with the program PLATON.^[31] The ring size, which is defined as the number of tetrahedral metal atoms, is 30.

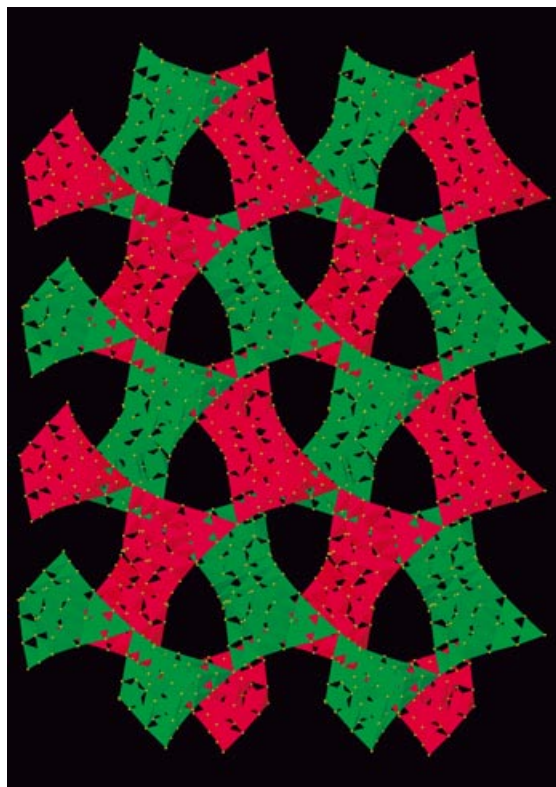


Figure 2. Three-dimensional framework of ICF-26. Red and green represent two interpenetrating diamond-type lattices.

One of the most prominent properties of ICF-26 is its fast ion conductivity. The specific conductivity is as high as $0.15 \Omega^{-1} \text{cm}^{-1}$ at 27°C under 100% relative humidity (RH) (Figure 3), which is significantly higher than that of other well-known crystalline lithium conductors at room temperature. Prior to our work, the highest conductivity for a crystalline lithium compound was about $10^{-3} \Omega^{-1} \text{cm}^{-1}$ at room temperature.^[23] The ionic conductivity of ICF-26 increases with increasing relative humidity. At about 26°C, the conductivity ranges from $0.011 \Omega^{-1} \text{cm}^{-1}$ at 29.8% RH to $0.15 \Omega^{-1} \text{cm}^{-1}$ under 100% RH (Figure 3). This property is potentially useful in electrochemical sensors.

The optical properties of ICF-26 were studied with solid-state diffuse reflectance UV/Vis–NIR spectroscopy. It showed a clear optical transition with a band gap of 3.51 eV (Figure 4). The transition is likely a result of charge transfer from the S^{2-} -dominated valence band to the $\text{In}^{3+}/\text{Li}^{+}$ -dominated conduction band. When excited at 375 nm at room

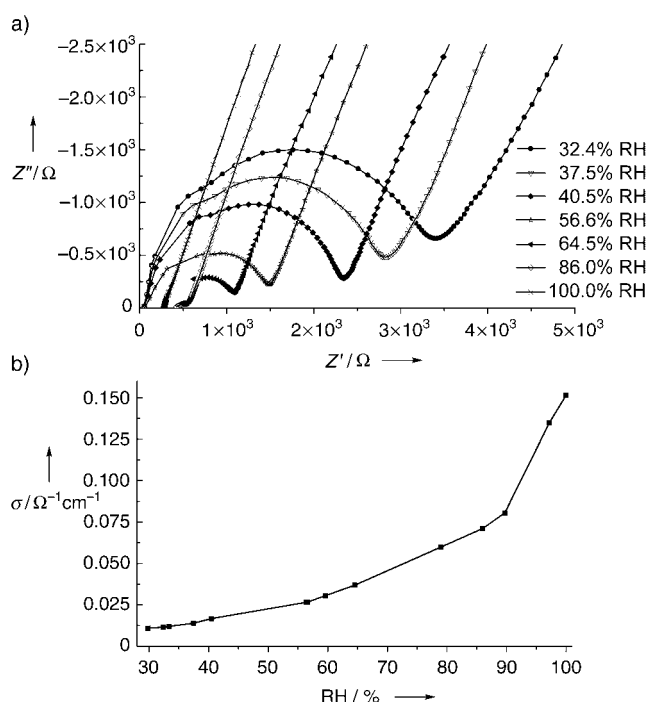


Figure 3. a) The ac impedance plots of ICF-26 at room temperature and different relative humidities. b) Ionic conductivity of ICF-26 at different relative humidities. Ionic conductivities were measured on a single crystal (cross section: $0.37 \times 0.43 \text{ mm}$, length: 0.63 mm) by the ac impedance method with a Solatron 1260 frequency response analyzer. The resistance decreased from $3.590 \times 10^3 \Omega$ at 29.8% RH to $2.614 \times 10^2 \Omega$ at 100% RH.

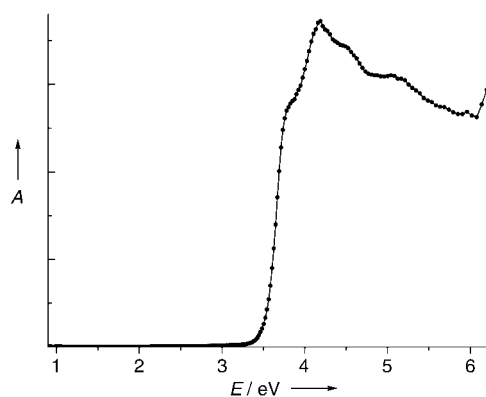


Figure 4. Optical absorption spectra of ICF-26. The absorption data were calculated from reflectance data by using the Kubelka–Munk function. BaSO_4 powder was used as a reference (100% reflectance). UV/Vis–NIR diffuse reflectance spectra were measured on a Shimadzu UV 3101PC double-beam, double-monochromator spectrophotometer. A = absorbance.

temperature, ICF-26 exhibits strong photoluminescence with the maximum wavelength centered at 440 nm.

In conclusion, the second member of a rare series of chalcogenide tetrahedral clusters ($\text{Li}_4\text{In}_{22}\text{S}_{44}^{18-}$) has been synthesized as the building block for a three-dimensional chalcogenide open-framework superlattice. The geometric features of the cluster can be simply described as the coupling

between four peripheral supertetrahedral clusters and one core antisupertetrahedral cluster. The highly mobile extra-framework cations lead to extraordinary humidity-dependent fast ion conductivity at room temperature.

Received: April 20, 2004

Keywords: cluster compounds · hydrothermal synthesis · indium · microporous materials · sulfur

- [1] V. N. Soloviev, A. Eichhöfer, D. Fenske, U. Banin, *J. Am. Chem. Soc.* **2001**, *123*, 2354–2364.
- [2] W. S. Sheldrick, M. Wachhold, *Angew. Chem.* **1997**, *109*, 214–233; *Angew. Chem. Int. Ed. Engl.* **1997**, *36*, 206–224.
- [3] B. Krebs, G. Henkel, *Angew. Chem.* **1991**, *103*, 785–804; *Angew. Chem. Int. Ed. Engl.* **1991**, *30*, 769–788.
- [4] I. Dance, K. Fisher, *Prog. Inorg. Chem.* **1994**, *41*, 637–803.
- [5] P. Behrens, G. D. Stucky in *Comprehensive Supramolecular Chemistry*, Vol. 7 (Eds.: J. L. Atwood, J. E. D. Davies, D. D. MacNicol, F. Vögtle, J.-M. Lehn, S. V. Ley), Pergamon, Oxford, **1996**, pp. 721–772.
- [6] T. Vossmeier, G. Reck, L. Katsikas, E. T. K. Haupt, B. Schulz, H. Weller, *Science* **1995**, *267*, 1476–1479.
- [7] E. M. Flanigen in *Introduction to Zeolite Science and Practice* (Eds.: H. van Bekkum, E. M. Flanigen, J. C. Jansen), Elsevier, New York, **1991**, pp. 13–34.
- [8] M. E. Davis, *Nature* **2002**, *417*, 813.
- [9] A. K. Cheetham, G. Férey, T. Loiseau, *Angew. Chem.* **1999**, *111*, 3466–3492; *Angew. Chem. Int. Ed.* **1999**, *38*, 3268–3292.
- [10] H. Li, A. Laine, M. O’Keeffe, O. M. Yaghi, *Science* **1999**, *283*, 1145–1147.
- [11] C. L. Cahill, J. B. Parise, *J. Chem. Soc. Dalton Trans.* **2000**, 1475–1482.
- [12] X. Bu, N. Zheng, Y. Li, P. Feng, *J. Am. Chem. Soc.* **2002**, *124*, 12646–12647.
- [13] N. Zheng, X. Bu, B. Wang, P. Feng, *Science* **2002**, *298*, 2366–2369.
- [14] $\text{In}(\text{NO}_3)_3 \cdot \text{H}_2\text{O}$ (0.3196) and Li_2S (0.2048 g) were mixed in water (1.0667 g) and stirred until a clear solution formed. CaCl_2 (0.2228 g) was then added to the solution and a cloudy gel mixture formed within minutes. The mixture was placed in a 23 mL autoclave and kept at 150 °C for 3 days. Large crystals of ICF-26 formed in about 30% yield. Crystallographic data for ICF-26: $\text{Ca}_{1.5}\text{Li}_{11}(\text{In}_{22}\text{Li}_4\text{S}_{42}) \cdot 44\text{H}_2\text{O}$, *Pbca*, $a = 28.172(4)$, $b = 29.183(4)$, $c = 40.0949(6)$ Å, $V = 32962(8)$ Å³, $Z = 8$, $\text{MoK}\alpha$, $T = 150$ K, $2\theta_{\text{max}} = 40^\circ$, $R(F) = 8.25\%$, $wR(F^2) = 19.6\%$ for 757 parameters and 15348 reflections with $I > 2\sigma(I)$, $R(F) = 13.9\%$, $wR(F^2) = 26.3\%$ for all data. Elemental analysis (%) found (calcd): Li 2.24 (2.16), Ca 1.23 (1.24), In 52.26 (52.30). Further details on the crystal structure investigations may be obtained from the Fachinformationszentrum Karlsruhe, 76344 Eggenstein-Leopoldshafen, Germany (fax: (+49)7247-808-666; e-mail: crysdata@fiz-karlsruhe.de), on quoting the depository number CSD-413961.
- [15] N. Herron, J. C. Calabrese, W. E. Farneth, Y. Wang, *Science* **1993**, *259*, 1426–1428.
- [16] A. Eichhöfer, D. Fenske, *J. Chem. Soc. Dalton Trans.* **2000**, 941–944.
- [17] G. B. Gardner, D. Venkataraman, J. S. Moore, S. Lee, *Nature* **1995**, *374*, 792.
- [18] B. Chen, M. Eddaouli, S. T. Hyde, M. O’Keeffe, O. M. Yaghi, *Science* **2001**, *291*, 1021.
- [19] R. L. Bedard, S. T. Wilson, L. D. Vail, J. M. Bennett, E. M. Flanigen in *Zeolites: Facts, Figures, Future. Proceedings of the 8th International Zeolite Conference* (Eds.: P. A. Jacobs, R. A. van Santen), Elsevier, Amsterdam, **1989**, p. 375.
- [20] S. Dhingra, M. G. Kanatzidis, *Science* **1992**, *258*, 1769–1772.
- [21] R. W. J. Scott, M. J. MacLachlan, G. A. Ozin, *Curr. Opin. Solid State Mater. Sci.* **1999**, *4*, 113–121.
- [22] N. Zheng, X. Bu, P. Feng, *Nature* **2003**, *426*, 428–432.
- [23] M. Murayama, R. Kanno, M. Irie, S. Ito, T. Hata, N. Sonoyama, Y. Kawamoto, *J. Solid State Chem.* **2002**, *168*, 140–148.
- [24] G. S. H. Lee, D. C. Craig, I. Ma, M. L. Scudder, T. D. Bailey, I. G. Dance, *J. Am. Chem. Soc.* **1988**, *110*, 4863–4864.
- [25] O. Palchik, R. G. Iyer, J. H. Liao, M. G. Kanatzidis, *Inorg. Chem.* **2003**, *42*, 5052–5054.
- [26] S. Dehnen, M. K. Brandmayer, *J. Am. Chem. Soc.* **2003**, *125*, 6618–6619.
- [27] H. Li, J. Kim, T. L. Groy, M. O’Keeffe, O. M. Yaghi, *J. Am. Chem. Soc.* **2001**, *123*, 4867–6868.
- [28] E. Zintl, A. Harder, B. Dauth, *Z. Elektrochem.* **1934**, *40*, 588–593.
- [29] D. Schmitz, W. Bronger, *Z. Anorg. Allg. Chem.* **1987**, *553*, 248–260.
- [30] J. Leal-Gonzalez, S. S. Melibary, A. J. Smith, *Acta Crystallogr. Sect. C* **1990**, *46*, 2017–2019.
- [31] A. L. Spek, *Acta Crystallogr. Sect. A* **1990**, *46*, C34.